Fabrication of Nanofibers with Uniform Morphology by Self-Assembly of Designed Peptides

Sachiko Matsumura,[b] Shinobu Uemura,[b] and Hisakazu Mihara*[a]

Abstract: Fabrication of controlled peptide nanofibers with homogeneous morphology has been demonstrated. Amphiphilic β-sheet peptides were designed as sequences of Pro-Lys-X_1-Lys-X_2-X_2-Glu-X_1-Glu-Pro. X_1 and X_2 were hydrophobic residues selected from Phe, Ile, Val, or Tyr. The peptide **FI** (X_1 = Phe; X_2 = Ile) self-assemble into straight fibers with 80–120 nm widths and clear edges, as examined by transmission electron microscopy (TEM) and atomic force microscopy (AFM). The fiber formation is performed in a hierarchical manner: β-sheet peptides form a protofibril, the protofibrils assemble side-by-side to form a ribbon, and the ribbons then coil in a left-handed fashion to make up a straight fiber. These type of fibers are formed from peptides possessing hydrophobic aromatic Phe residue(s). Furthermore, a peptide with Ala residues at both N and C termini does not form fibers (100 nm scale) with clear edges; this causes random aggregation of small pieces of fibers instead. Thus, the combination of unique amphiphilic sequences and terminal Pro residues determine the fiber morphology.

Keywords: Beta-sheet · fiber · nanostructures · peptides · self-assembly

Introduction

Fabrication of nanoscale structures is one of the key goals in creating materials with extensive applications in nanotechnology. For nanofabrication, molecular self-assembly is promising as a bottom-up approach. Natural organisms are rich in sophisticated materials built in a self-assembling manner, and materials with a natural basis are needed for ecological reasons. Many researchers have attempted to exploit the self-assembling properties of proteins and peptides for materials directed towards nanodevices, tissue engineering, and so forth.[1–12] In fibrous proteins and peptides, which mainly consist of a β-sheet conformation, numerous β-strands are organized to form fibrous structures in a regular manner. Although β-sheet fibers are candidates for materials,[1–6] engineered β-sheet peptides generally tend to form aggregates with multiple morphologies such as bundled fibers or gels.[3,4] Typical sequences of designed β-sheet peptides have regular repeats of alternating hydrophobic and hydrophilic residues.[3,4,13,14] These sequences will make an amphiphilic binary pattern [14] (two distinct surfaces of hydrophobic and hydrophilic) in β-strands. The hydrophobic and complementary ionic interactions provide driving forces for the formation of β-strand assemblies together with hydrogen bonding.[3–5] A variety of β-sheet peptides with an alternating hydrophobic and hydrophilic pattern were systematically designed by Zhang and co-workers, and the structures and gel formation behaviors were characterized in relation to the hydrophobic and ionic residues.[3] In order to exploit a single fiber and the alignment of β-strands within as a nanoscale material, preventing gel formation and controlling the fiber morphology are important procedures. With this aim, artificial short peptides are advantageous, because of the ease in strategic design of integrated or hybrid materials. Here, we describe the fabrication of controlled nanofibers through self-assembly of simple de novo designed β-sheet peptides with ten amino acid residues. As a result, homogeneous straight fibers with defined edges have been formed with a uniform morphology.

[a] Prof. H. Mihara
Graduate School of Bioscience and Biotechnology
Tokyo Institute of Technology, 4259 Nagatsuta-cho
Midori-ku, Yokohama 226-8501 (Japan)
Fax: (+81) 45-924-5833
E-mail: hmihara@bio.titech.ac.jp

[b] Dr. S. Matsumura, Dr. S. Uemura
Ecology Research Laboratory, Corporate Research
Laboratory, Fuji Xerox Co. Ltd., 430 Sakai, Nakai-machi
Ashigarakami-gun, Kanagawa 259-0157 (Japan)

Results and Discussion

Peptide design and fiber fabrication: We designed amphiphilic β-sheet peptides composed of ten residues: Pro-Lys-X_1-Lys-X_2-X_2-Glu-X_1-Glu-Pro (Figure 1). X_1 and X_2 were hydrophobic residues selected from Phe, Ile, Val, or Tyr. Lys and Glu were used as hydrophilic residues. Many of de novo

 DOI: 10.1002/chem.200305735

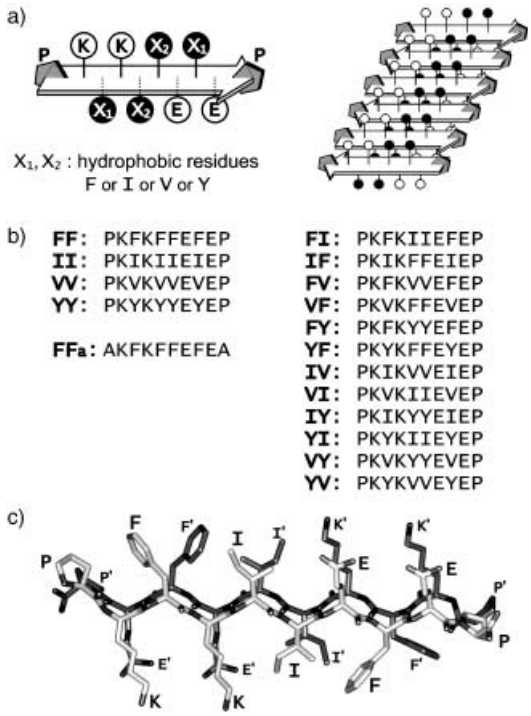

Figure 1. Design of the β-sheet peptides; a) illustration of a designed β-strand and a β-sheet structure composed of β-strands. Black and white balls represent hydrophobic and hydrophilic residues, respectively. For hydrophobic amino acid residues, one or two kinds of amino acids are selected from Phe (F), Ile (I), Val (V), or Tyr (Y). Hydrophilic residues are Lys (K) and Glu (E); b) amino acid sequences of the designed β-strand; c) molecular drawing of two strands of **FI** peptides aligned as an antiparallel β-sheet. The amino acid sequence of the strand (PKFKIIEFEP) is indicated, and the amino acids in the other strand are indicated as letters with prime. The structure was generated by using the Insight II/Discover program.

designed β-sheet peptides with a standard amphiphilic binary pattern easily aggregate to form bundles or gels of assembled peptides, which show various morphologies. The broad hydrophobic or charged faces of β-strands can increase the possibility for varied arrangements of β-strands including a staggered arrangement. For example, the peptide acetyl-Phe-Lys-Phe-Glu-Phe-Lys-Phe-Glu-amide appeared to form left-handed helical ribbon intermediates, and the the helical ribbons further bundled and formed a network towards a gel matrix.[3a,c] To reduce this unfavorable possibility, in this study, the hydrophobic and hydrophilic planes were divided, and the order was inverted at the center of the strand. Additionally, the charged Lys and Glu residues were arranged so as to generate electrostatic attraction in an antiparallel strand orientation, but repulsion in a parallel orientation. Moreover, in order to cut the hydrogen-bonding network in the β-sheet structure at the strand ends, we employed Pro residues at both N and C termini. The Pro residue does not have an N–H available for hydrogen bonding by virtue of the ring structure, and often acts as a β-sheet breaker.[15] Pro has the ability to reduce β-sheet expansion and extra fibril formation by stopping extension of the hydrogen-bonding network.[16,17] In the case of Pro residues placed at the strand termini, they could contribute to form two-dimensionally ordered β-sheet monolayers at the air–water interface.[18] Terminal Pro residues in our design were also expected to stop the unfavored hydrogen-bonding network by aligning at the rim of the assembled β-sheets. The above features potentially provided appropriate restrictions upon the assembly process by regulating hydrophobic and hydrophilic interactions and hydrogen-bonding ability (Figure 1).

All peptides were synthesized by standard 9-fluorenylmethyloxycarbonyl (Fmoc) solid-phase method, and purified by reversed-phase HPLC.[19] The peptides were identified by matrix-assisted laser desorption ionization time-of-flight mass spectrometry (MALDI-TOFMS) and amino acid analyses. For fabrication of fibers, peptides were dissolved at a concentration of 50–200 μM in a sodium phosphate buffer (0.1 M, pH 7.4), and the solutions were allowed to stand at room temperature for over 24 hours.

Fiber morphology studied by TEM and AFM: For investigation of fiber morphology, transmission electron microscopy (TEM) and atomic force microscopy (AFM) were used. The peptide **FI** (X_1 = Phe; X_2 = Ile) formed homogeneous straight fibers with clear edges, 80–130 nm in width and ~10 μm in length (Figure 2a and b). In the fine structure of the straight fiber, striations of about 10 nm width crossing each other were observed (Figure 2c). Additionally, we observed fibers with a different morphology, namely a helical ribbon. In the ribbon, striations were also observed parallel to the ribbon edges (Figure 2d). The helical ribbon appeared to densely coil, and then grow into a straight fiber (Figure 2e).

AFM images of the **FI** fibers resembled those visualized by TEM (Figure 3). The **FI** fibers were 80–120 nm in width and had inner striations with 10–15 nm intervals (Figure 3a and b). The height of straight fibers was 2–8 nm. The 3D image of **FI** apparently showed a left-handed coiled ribbon (Figure 3c). In the helical ribbons, the lower layer was 2–4 nm in height and the upper layer was 5–8 nm, approximately double that of the lower. These results strongly support the idea mentioned above that the straight fibers with clear edges were formed from tightly coiled ribbons.

This type of fiber was also formed from peptides other than **FI**. **IF** (X_1 = Ile; X_2 = Phe), **FV** (X_1 = Phe; X_2 = Val), and **VF** (X_1 = Val; X_2 = Phe) all formed helical ribbons and straight fibers with striations as successfully as **FI**. These peptides substantially showed the same morphologies as **FI** in respect of the straight fibers and coiled ribbons (including the width). The straight fibers made from tightly coiled ribbons were most frequently observed in the case of **FI**. The peptide **FF** (X_1 = Phe; X_2 = Phe) formed wider fibers (100–250 nm in width) with similar inner striations, or in some cases formed a film-like structure with ~500 nm width (Figure 4a).

On the other hand, peptides with only aliphatic side chains in the hydrophobic residues showed fibers with a very different morphology. The peptides **VI** (X_1 = Val; X_2 = Ile), **IV** (X_1 = Ile; X_2 = Val), and **II** (X_1 = Ile; X_2 = Ile) formed straight fibers, but these appeared to have a tape-like morphology (Figure 4b). The tape-like fibers did not

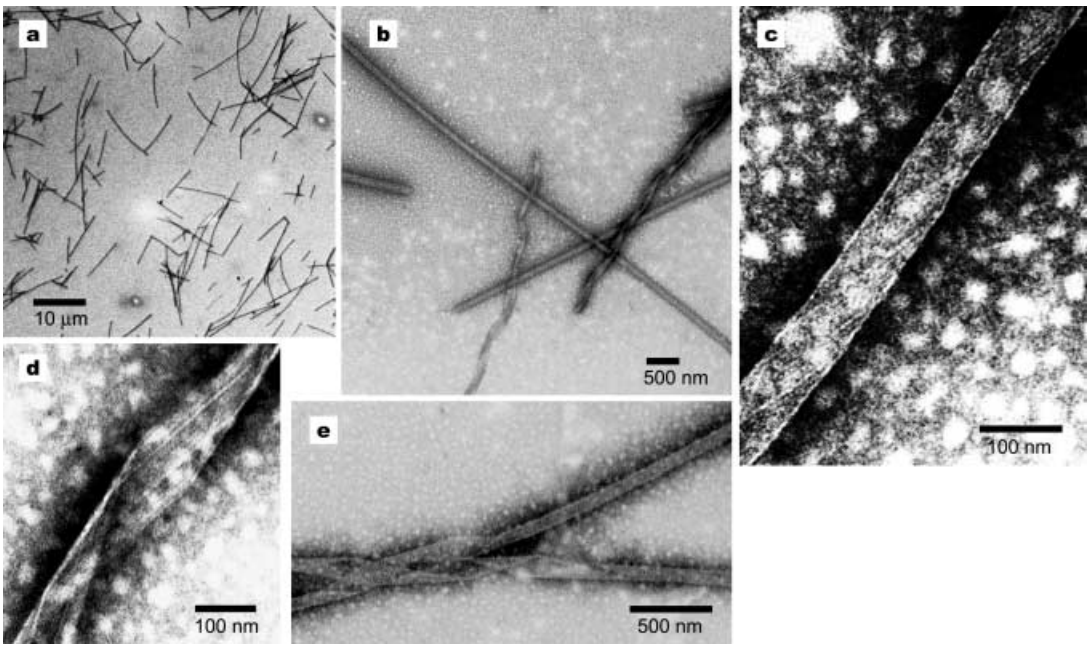

Figure 2. TEM images of **FI** fibers; a) macro image shows a uniform morphology of fibers; b) both straight fibers and helical ribbons are shown. Straight fibers have clear edges and a uniform width; c) high magnification of the straight fiber shows crossed striations within. The intervals of the striations are uniform; d) observed striations in the ribbon are parallel to the ribbon edges; e) each helical ribbon gradually changes to a straight fiber.

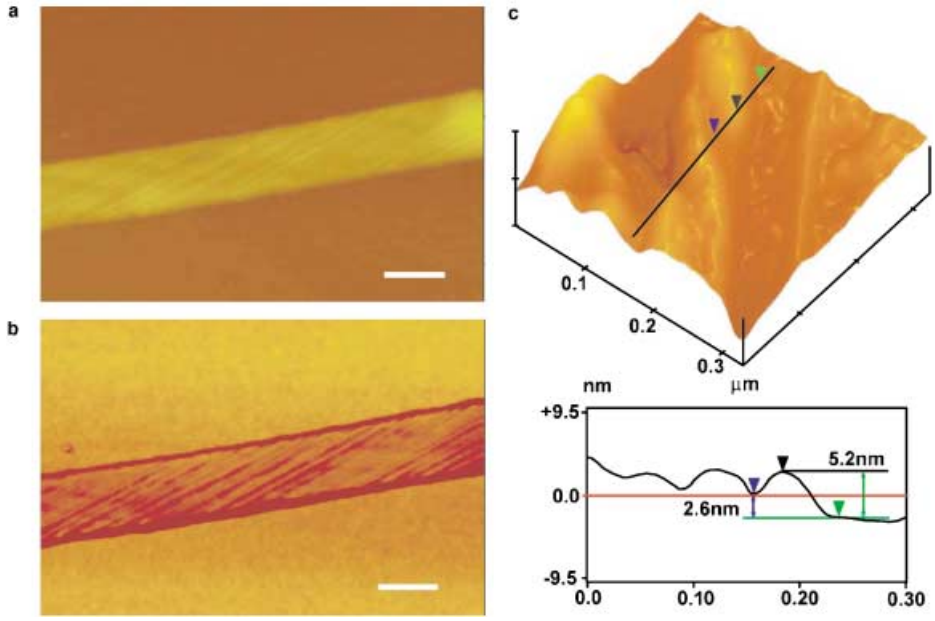

Figure 3. Tapping-mode AFM images of **FI** fibers on HOPG in ambient conditions, scale bars = 100 nm; a) height and b) phase images show inner striations; c) the 3D image shows a left-handed helically coiled fiber.

coil and were laterally associated into wider tapes of variable width (100–500 nm). No crossed striation was observed in these fibers, and in this regard, they were distinctly different from **FI** fibers.

Thus, the peptides that formed helical ribbons and straight fibers with striations had hydrophobic aromatic Phe residues. Moreover, the combination of aromatic and aliphatic side chains seemed to promote regular formation of coiled fibers. Peptides with one or two hydrophobic Tyr residues did not form fibers, despite having an aromatic side chain.

Structural analyses by CD: The circular dichroism (CD) studies revealed that all peptide fibers had a β-sheet structure. Especially, CD spectra of **FI** imply a strongly twisted β-sheet structure. CD spectra at pH 7.4 showed a negative maximum around 221 nm ($[\theta]_{221} = -6500\ \mathrm{deg\,cm^2\,dmol^{-1}}$, immediately after sample preparation), and a positive maximum near 202 nm ($[\theta]_{202} = 11\,400\ \mathrm{deg\,cm^2\,dmol^{-1}}$), characteristic of a β-sheet structure (Figure 5a). The CD signal intensity increased with time (from −6500 to $-9300\ \mathrm{deg\,cm^2\,dmol^{-1}}$ at 221 nm, from 11 400 to $123\,600\ \mathrm{deg\,cm^2\,dmol^{-1}}$ at 202 nm), which indicated spontaneous fiber formation. In the case of **FI**, the π–π* band (202 nm) became much stronger than the n–π* band (221 nm) upon incubation. The ratio of signal values of π–π* to n–π* ($|[\theta]_{202}|/|[\theta]_{221}|$) was greater than 13, significantly larger than 4.1 for **VI** (Figure 5a and b). The CD results for the peptide **FI** indicate a strongly twisted β-sheet structure.[20] The structure preferentially induces formation of

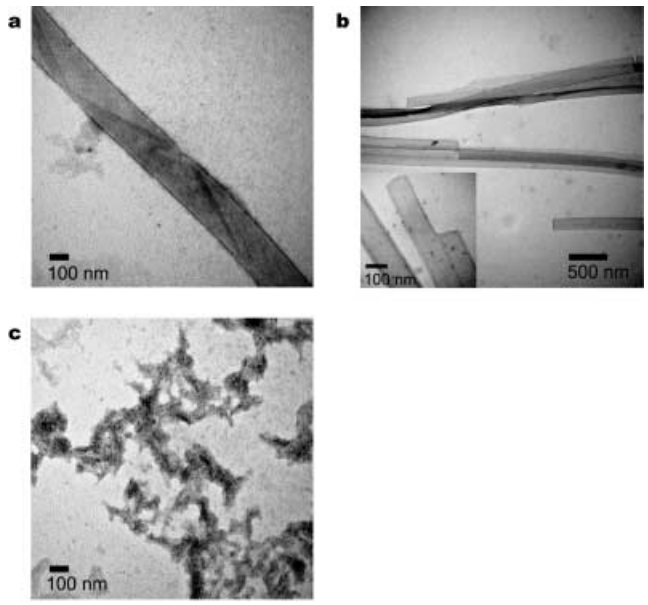

Figure 4. TEM images of **FF** and **VI** fibers; a) the **FF** fiber with terminal Pro residues has a large width and clear edges; b) the **VI** fibers do not coil. These tape-like fibers associate side-by-side into fibers of variable width. The inset shows no crossed striations in the tape-like fibers; c) the image of fibers formed from **FF** with Ala residues at both termini (**FFa**) shows disordered aggregation of small pieces.

straight fibers with striations at uniform interval resulting from helical ribbons.

In contrast to a neutral pH range, at pH 2 and pH 11, the CD spectra of **FI** corresponded to those of an almost random structure and did not change with time (Figure 5c and d). After a week, no fibers were observed by TEM. The addition of NaCl to the peptide solutions at pH 7.4 also suppressed the β-sheet and fiber formation (Figure 5e). These results suggest that the electrostatic interaction between Glu and Lys is important for fiber formation at neutral pH. At extreme pH values, repulsions between charged peptides possibly inhibit the aggregation. In the designed peptide, Glu and Lys can interact with each other in a complementary manner when the β-strands are arranged in an antiparallel orientation (Figure 1); this suggests the fiber might have an antiparallel β-sheet structure.[5]

Effect of terminal Pro residues on fiber morphology: Formation of straight fibers was supposedly attributed to the Pro residues at both the N and C termini, because fibers (100 nm) with clear edges were not found in a peptide with Ala residues at both termini. The Ala-containing peptide (**FFa**) caused random aggregation of many small pieces of fiber (Figure 4c). This aggregation was not regarded as a "single" fiber with clear edges, and was apparently different from the fibers of peptides with Pro residues (Figure 2 and Figure 4a). The difference suggests that the Pro residues at both N and C termini contribute to controlled fiber formation. The Pro residue has a cyclic side chain and lacks the hydrogen-bond donor. The *N*-alkylated amino acids have the ability to act as β-sheet breakers, and the fibrillar or gel formation can be suppressed by peptides with these residues

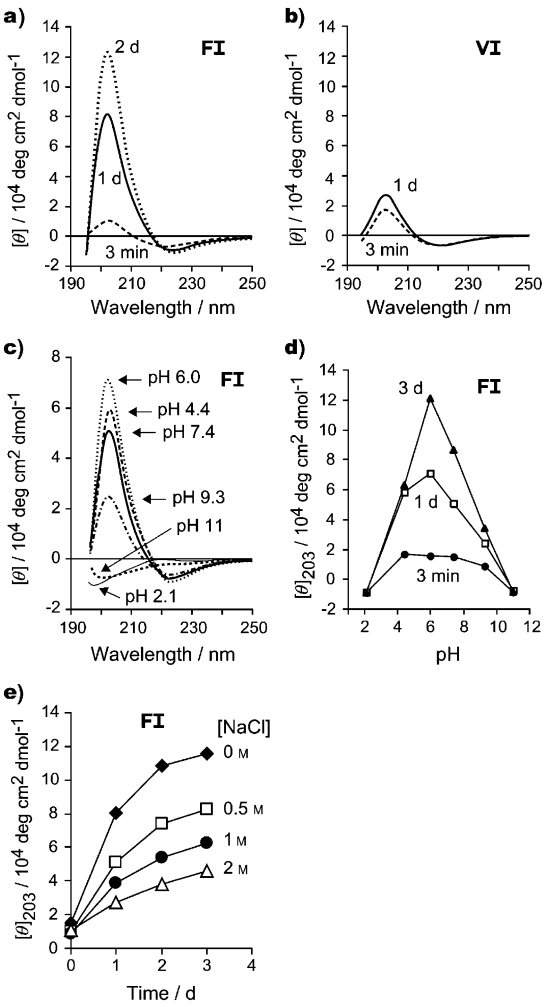

Figure 5. CD spectra of the β-sheet peptides. CD spectral change of a) **FI** and b) **VI** as a function of time. The CD signal at 202 nm for **FI** increased significantly compared with that for **VI**. [**FI**] = 100 μM, [**VI**] = 200 μM in 0.1 M sodium phosphate buffer (pH 7.4) at 25 °C; c) pH-dependent change of CD spectrum of **FI**. Each **FI** solution in the pH range of 2.1 to 11 was measured after incubation for a day. The CD spectra were characteristic of a β-sheet structure between pH 4.4 and pH 9.3. At pH 2.1 and pH 11 the peptide was shown to exist in an almost random structure; d) the CD signals at 203 nm versus pH values were plotted as a function of time. The signal increase was shown in a neutral pH range; e) NaCl concentration dependency of fiber formation. Fiber formation of **FI** was performed in the buffer at pH 7.4 with various concentrations of NaCl. The CD signals at 203 nm were reduced with increasing concentrations of NaCl.

within the strand.[16,17] The extent of the hydrogen-bonding network of β-sheet structures can be stopped at positions of the Pro residues. A previous report showed the effect of Pro residues at the strand termini on β-sheet association. The peptides of a standard amphiphilic binary pattern, with Pro residues at both termini (sequence Pro-Glu-(Phe-Glu)*n*-Pro), formed a crystalline β-sheet monolayer at the air–water interface.[18] In the monolayer, the β-strands were ordered two-dimensionally by distinct chain termini of Pro. In this context, terminal Pro residues appeared to have the potential to determine the manner of β-sheet association by aligning at the rim of assembled β-sheets. In our designed peptides, terminal Pro residues could function effectively.

Effect of hydrophobic residues on fiber formation: CD studies revealed that the ability to form a β-sheet structure was dependent on the hydrophobic residues. The order of the ability was **II** > **FF** > **IF** ≥ **FI** ≫ **VI** ≥ **IV** ≥ **FV** ≥ **VF**. **VV** and peptides with one or two hydrophobic Tyr residues did not form fibers. The Tyr residue is not among the most hydrophobic of the amino acids, whilst the order of amino acid preference for β-sheet formation is Val > Ile > Tyr > Phe.[15] These results imply that fiber formation is affected not only by the tendency for β-sheet formation, but also by the hydrophobic nature of amino acids constituting the peptide sequence. Fiber morphology seems to be delicately determined by the interactions between hydrophobic residues. The peptides with aromatic Phe residues formed helical ribbons and straight fibers with striations, in contrast with the fibers without striations assembled from **II**, **VI**, and **IV**. One significant factor would be the aromatic interaction between Phe residues in β-strands. These interactions play a significant role in molecular recognition and self-assembly, and can provide a contribution to an ordered structure in fibrous peptides and proteins.[21] The dipeptide Phe-Phe was reported to form a tubular structure,[21a] which directly indicated the importance of the aromatic interaction for structure formation. The fiber formation shown in this study was also largely attributed to the interaction between Phe residues. Additionally, the combination of aromatic and aliphatic side chains in hydrophobic residues, represented in the sequence of **FI**, promotes strongly twisted β-sheets towards a unique tertiary structure.

Hierarchical fiber formation: CD studies confirm that the peptide fibers have a β-sheet structure, probably in an antiparallel strand orientation. Furthermore, Congo red, a dye which binds to fibrous peptides with a cross β-sheet conformation,[22] was effectively bound to the peptides. These results indicate that the fibers contain a structure common to that of other reported fibrous peptides and proteins with a β-sheet structure.[22–24] Fluorophore specifically bound to amyloid fibrils, thioflavin T, and did not show a remarkable increase of fluorescence.[25] Thus, the peptide fibers are different from fibrils called amyloids. The fibrous peptides and proteins self-assemble in a hierarchical manner, and peptide β-sheets assemble to form protofibrils; these then associate into higher ordered fibrillar assemblies.[3c,4,26] The reported protofibrils are 5–17 nm in width,[3c,4e,26–29] and almost coincident with that of the striations in **FI** fibers (Figure 2 and 3). This coincidence implies that protofibrils, like those reported, are initially formed from the peptide **FI**. The protofibrils align side-by-side to make up a ribbon, and then the ribbons helically coil to form straight fibers with a width of 100 nm. The straight fibers exist as a "single" fiber, and intertwisting or bundling can be suppressed.

Regular strand alignment contributes to fiber formation with uniform morphology. The strand alignment was enhanced by terminal Pro residues and the short length of the unique binary pattern. The order of hydrophilic and hydrophobic residues was reversed at the center of the strand. This pattern allowed both hydrophobic and hydrophilic interfaces on each side of a β-strand, and the narrow interfaces were capped by Pro residues incapable of hydrogen bonding. Pro residues ordered β-strands by aligning at the rim of β-sheets. Hydrophobic and electrostatic interactions on both sides of a β-sheet were available for precise recognition between the sheets, and the interactions worked most effectively when the β-strands were in a regular unstaggered arrangement (Figure 1). Electrostatic attractions are generated in antiparallel β-strand assemblies, and aromatic interactions between Phe residues easily function simultaneously. In the case of **FI**, particular recognition surfaces are anticipated to be created by a combination of aromatic and aliphatic side chains in hydrophobic residues. The recognition induces the strongly twisted β-sheet structure, which facilitates the formation of helical ribbons tightly coiled. Thereby, uniform straight fibers with clear edges are fabricated. Optimization of the interactions, including hydrogen bonds, is advantageous for making defined β-sheet assemblies.

Conclusion

Fabrication of nanoscale fibers with homogeneous morphology was accomplished by self-assembly of designed β-sheet peptides. The peptides formed straight fibers with uniform width and clear edges. The morphology could be controlled by peptide design: a unique amphiphilic binary pattern, Pro residues at both N and C termini and a combination of hydrophobic residues. Nanofibers with an ordered structure of self-assembled peptides can potentially be developed as biodegradable materials for applications in nanotechnology.

Experimental Section

Peptide synthesis: Peptides were synthesized by the solid-phase method by using Fmoc strategy[19] on Advanced Chemtech BenchMark model 348 multiple peptide synthesizer by means of the following Fmoc–amino acid derivatives: Fmoc-Ala-OH, Fmoc-Glu(O*t*Bu)-OH, Fmoc-Ile-OH, Fmoc-Lys(Boc)-OH, Fmoc-Phe-OH, Fmoc-Pro-OH, Fmoc-Tyr(*t*Bu)-OH, and Fmoc-Val-OH (*t*Bu; *tert*-butyl, Boc; *tert*-butyloxycarbonyl) The peptide chains were assembled on a 2-chlorotrityl chloride resin by using Fmoc–amino acid derivatives (3 equiv), *N,N*-diisopropylethylamine (DIEA, 6 equiv), 2-(1H-9-azabenzotriazole-1-yl)-1,1,3,3-tetramethyluronium hexafluorophosphate (HATU, 3 equiv) in *N*-methylpyrrolidone (NMP) for coupling, and piperidine (25%) (PPD)/NMP for Fmoc removal. To cleave the peptide from the resin and remove the side chain protecting groups, the peptide–resin was treated with trifluoroacetic acid (TFA)/triisopropylsilane/water (95:2.5:2.5). All peptides were purified by semi-preparative RP-HPLC on a COSMOSIL 5C18-AR-300 packed column (10 × 250 mm) by using a linear gradient of acetonitrile/0.1% TFA at a flow rate of 3.0 mL min^{-1}. The peptides were identified satisfactorily by matrix-assisted laser desorption ionization time-of-flight mass spectrometry (MALDI-TOFMS) and amino acid analyses. MALDI-TOFMS was performed on a Shimadzu KOMPACT MALDI III mass spectrometer by using 3,5-dimethoxy-4-hydroxycinnamic acid as a matrix. Amino acid analyses were carried out by using a Wakopak WS-PTC column (4.0 × 200 mm) after hydrolysis in HCl (6 M) at 110 °C for 24 h in a sealed tube, and labeling by phenylisothiocyanate (PITC).

Preparation of peptide fibers: For peptide stock solutions, peptides were dissolved at a concentration of 2 mM in 15% ethanol/water containing TFA (0.1%). For fabrication of fibers, peptides were diluted to a concentration of 50–200 μM with sodium phosphate buffer (0.1 M, pH 7.4), and the solutions were allowed to stand at room temperature for over 24 hours.

CD: CD measurements were performed on a J-720WI spectropolarimeter at 25 °C by using a quartz cell with 1.0 mm pathlength. Peptide solution was prepared by diluting a stock solution with sodium phosphate buffer (0.1 M). Immediately after the dilution the measurement was started.

TEM: Collodion-coated copper EM grids were placed coated-side down onto the peptide solution for 30 seconds, and excess solution was removed by blotting with filter paper. The grids were washed by floating on water and water was removed by blotting. The sample was negatively stained with 2 % (w/v) phosphotungstic acid for 30 seconds. The grids were blotted and allowed to dry gradually at room temperature. All images were taken by using a Hitachi H-7500 electron microscope operating at 100 kV.

AFM: Tapping-mode AFM observations were carried out by Nanoscope IIIa AFM, Dimension 3000 (Digital Instruments, Santa Barbara, CA, USA) in ambient conditions. AFM samples were prepared by spreading the peptide solutions on highly oriented pyrolytic graphite (HOPG), and dried under vacuum after removal of excess solution.

[1] *Self-Assembling Peptide Systems in Biology, Medicine and Engineering*, (Eds.: A. Aggeli, N. Boden, S. Zhang), Kluwer Academic Publishers, Dordrecht, **2001**.

[2] S. Zhang, D. M. Marini, W. Hwang, S. Santoso, *Curr. Opin. Chem. Biol.* **2002**, *6*, 865–871.

[3] a) M. R. Caplan, E. M. Schwartzfarb, S. Zhang, R. D. Kamm, D. A. Lauffenburger, *Biomaterials* **2002**, *23*, 219–227; b) T. C. Holmes, S. de Lacalle, X. Su, G. Liu, A. Rich, S. Zhang, *Proc. Natl. Acad. Sci. USA* **2000**, *97*, 6728–6733; c) D. M. Marini, W. Hwang, D. A. Lauffenburger, S. Zhang, R. D. Kamm, *Nano Lett.* **2002**, *2*, 295–299; d) M. Altman, P. Lee, A. Rich, S. Zhang, *Protein Sci.* **2000**, *9*, 1095–1105.

[4] a) A. Aggeli, M. Bell, N. Boden, L. M. Carrick, A. E. Strong, *Angew. Chem.* **2003**, *115*, 5761–5764; *Angew. Chem. Int. Ed.* **2003**, *42*, 5603–5606; b) A. Aggeli, M. Bell, L. M. Carrick, C. W. G. Fishwick, R. Harding, P. J. Mawer, S. E. Radford, A. E. Strong, N. Boden, *J. Am. Chem. Soc.* **2003**, *125*, 9619–9628; c) A. Aggeli, M. Bell, N. Boden, J. N. Keen, P. F. Knowles, T. C. B. McLeish, M. Pitkeathly, S. E. Radford, *Nature* **1997**, *386*, 259–262; d) A. Aggeli, I. A. Nyrkova, M. Bell, R. Harding, L. Carrick, T. C. B. McLeish, A. N. Semenov, N. Boden, *Proc. Natl. Acad. Sci. USA* **2001**, *98*, 11857–11862; e) C. W. G. Fishwick, A. J. Beevers, L. M. Carrick, C. D. Whitehouse, A. Aggeli, N. Boden, *Nano Lett.* **2003**, *3*, 1475–1479.

[5] a) Y. Takahashi, A. Ueno, H. Mihara, *ChemBioChem* **2002**, *3*, 637–642; b) Y. Takahashi, A. Ueno, H. Mihara, *ChemBioChem* **2001**, *1*, 75–79.

[6] T. Scheibel, R. Parthasarathy, G. Sawicki, X.-M. Lin, H. Jaeger, S. L. Lindquist, *Proc. Natl. Acad. Sci. USA* **2003**, *100*, 4527–4532.

[7] J. D. Hartgerink, E. Beniash, S. I. Stupp, *Science* **2001**, *294*, 1684–1688.

[8] Z. Li, S.-W. Chung, J.-M. Nam, D. S. Ginger, C. A. Mirkin, *Angew. Chem.* **2003**, *115*, 2408–2411; *Angew. Chem. Int. Ed.* **2003**, *42*, 2306–2309.

[9] M. Knez, A. M. Bittner, F. Boes, C. Wege, H. Jeske, E. Maiß, K. Kern, *Nano Lett.* **2003**, *3*, 1079–1082.

[10] R. A. Mcmillan, C. D. Paavola, J. Howard, S. L. Chan, N. J. Zaluzec, J. D. Trent, *Nat. Mater.* **2002**, *1*, 247–252.

[11] H. A. Lashuel, S. R. LaBrenz, L. Woo, L. C. Serpell, J. W. Kelly, *J. Am. Chem. Soc.* **2000**, *122*, 5262–5277.

[12] M. G. Ryadnov, B. Ceyhan, C. M. Niemeyer, D. N. Woolfson, *J. Am. Chem. Soc.* **2003**, *125*, 9388–9394.

[13] W. F. DeGrado, C. M. Summa, V. Pavone, F. Nastri, A. Lombardi, *Annu. Rev. Biochem.* **1999**, *68*, 779–819.

[14] a) M. W. West, M. H. Hecht, *Protein Sci.* **1995**, *4*, 2032–2039; b) M. W. West, W. Wang, J. Patterson, J. D. Mancias, J. R. Beasley, M. H. Hecht, *Proc. Natl. Acad. Sci. USA* **1999**, *96*, 11211–11216; c) G. Xu, W. Wang, J. T. Groves, M. H. Hecht, *Proc. Natl. Acad. Sci. USA* **2001**, *98*, 3652–3657.

[15] P. Y. Chou, G. D. Fasman, *Annu. Rev. Biochem.* **1978**, *47*, 251–276.

[16] D. F. Moriarty, D. P. Raleigh, *Biochemistry* **1999**, *38*, 1811–1818.

[17] D. T. S. Rijkers, J. W. M. Höppener, G. Posthuma, C. J. M. Lips, R. M. J. Liskamp, *Chem. Eur. J.* **2002**, *8*, 4285–4291.

[18] H. Rapaport, K. Kjaer, T. R. Jensen, L. Leiserowitz, D. A. Tirrell, *J. Am. Chem. Soc.* **2000**, *122*, 12523–12529.

[19] W. C. Chan, P. D. White, in *Fmoc Solid Phase Peptide Synthesis: A Practical Approach* (Eds.: W. C. Chan, P. D. White), Oxford University Press, New York, **2000**, pp. 41–76.

[20] R. W. Woody, in *Circular Dichroism and the Conformational Analysis of Biomolecules* (Ed.: G. D. Fasman), Plenum, New York, **1996**, pp. 25–67.

[21] a) M. Reches, E. Gazit, *Science* **2003**, *300*, 625–627; b) E. Gazit, *FASEB J.* **2002**, *16*, 77–83.

[22] W. E. Klunk, R. F. Jacob, R. P. Mason, *Anal. Biochem.* **1999**, *266*, 66–76.

[23] S. J. Wood, B. Maleeff, T. Hart, R. Wetzel, *J. Mol. Biol.* **1996**, *256*, 870–877.

[24] J. R. Glover, A. S. Kowal, E. C. Schirmer, M. M. Patino, J.-J. Liu, S. Lindquist, *Cell* **1997**, *89*, 811–819.

[25] H. LeVine III, *Methods Enzymol.* **1999**, *309*, 274–284.

[26] N. M. Kad, S. L. Myers, D. P. Smith, D. A. Smith, S. E. Radford, N. H. Thomson, *J. Mol. Biol.* **2003**, *330*, 785–797.

[27] C. Goldsbury, K. Goldie, J. Pellaud, J. Seelig, P. Frey, S. A. Müller, J. Kistler, G. J. S. Cooper, U. Aebi, *J. Struct. Biol.* **2000**, *130*, 352–362.

[28] T. S. Burkoth, T. L. S. Benzinger, V. Urban, D. M. Morgan, D. M. Gregory, P. Thiyagarajan, R. E. Botto, S. C. Meredith, D. G. Lynn, *J. Am. Chem. Soc.* **2000**, *122*, 7883–7889.

[29] O. S. Makin, L. C. Serpell, *Biochem. Soc. Trans.* **2002**, *30*, 521–525.

Received: November 20, 2003
Revised: February 6, 2004

Published online: April 22, 2004